



Landuse classification of hyperspectral data by spectral angle mapper and support vector machine in humid tropical region of India

Girish Gopinath^{1,2} · Nimmi Sasidharan¹ · U. Surendran³

Received: 19 September 2019 / Accepted: 11 December 2019 / Published online: 4 January 2020
© Springer-Verlag GmbH Germany, part of Springer Nature 2020

Abstract

Hyperspectral images are being used in various fields. The main objective of the present study was to use hyperspectral imagery from Hyperion with Spectral Angle Mapper (SAM) and Support Vector Machine (SVM) for discriminating the landuse/landcover classes in Kozhikode district, Kerala which constitutes a combination of different physiographic land features. Hyperion functions from a space platform with modest surface signal levels and a full column of atmosphere persuading the signal, hence, the data derived from this demand careful pre-processing to minimize sensor and atmospheric noise. The atmospheric correction using MODTRAN based FLAASH module as well as the data dimensionality reduction by Principal Component Analysis (PCA) made the Hyperion to allow discrete reflectance values. Advanced classifiers like SAM and SVM could describe the pattern and spatial distribution of landcover. From the accuracy assessments, SVM showed better classified result than SAM with overall accuracy 85.6% and kappa coefficient 0.89. This study suggests that SVM can be used for landuse/landcover classification of hyperspectral data with high accuracy.

Keywords Hyperion · FLAASH module · Geometric correction · Landuse/landcover · PCA · SVM and SAM

Introduction

Satellites have been launched to move ahead in our understanding on Earth's environment. These active and passive satellite sensors imprint data ranging from visible to microwave regions of electromagnetic spectrum. A broad range of satellites, such as Moderate Resolution Imaging Spectroradiometer (MODIS); Landsat Thematic Mapper and Enhanced Thematic Mapper (TM/ETM+); Global Imager (GLI); ResourceSAT; Advanced Land Imager (ALI) and Hyperion, are often used in different fields viz., agriculture,

geology, forest, water resources, marine studies, atmospheric analysis, climatological/ meteorological and surveillance studies (Liu et al. 2009) and these are of multispectral / hyperspectral in nature. In general, multispectral remote sensing data have been used worldwide for various applications. However, one of the major limitations of the multispectral data is that the sensors function in range of wider wavelength bands thus have restrictive amount of spectral information available.

However, hyperspectral remote sensing is the quickly emerging and promising technology in the field of remote sensing. The major advantage of hyperspectral data is it is having a wider range of remote sensing applications by giving plentiful information than the conventional multispectral data. Hyperspectral images give a absolute depiction of the response of the surfaces, generally in the visible and infrared range. These sets of data permitus to supervise the processes happening at the surface in a non-intrusive way, whatever may be the scale i.e., both at the regional (micro), national and even at global level (macro level) (Lillesand et al. 2009).

Hyperspectral imaging sensors are skillful enough for giving robust variations of spectra for the materials in the surface, using the signatures obtained from numerous contiguous spectral channels in the entire visible-to-near infrared (VNIR) regions of the electromagnetic spectrum, which in turn help to

Communicated by: H. Babaie

✉ U. Surendran
suren@cwrmdm.org

¹ Geomatics Division, Centre for Water Resources Development and Management (CWRDM), Kozhikode, Kerala 673571, India

² Present address: Department of Remote Sensing and GIS, Kerala University of Fisheries and Ocean Studies, Kochi, Kerala, India

³ Water Management (Agriculture) Division, Centre for Water Resources Development and Management (CWRDM), Kozhikode, Kerala 673571, India

distinguish those materials from one another. The bands are very narrow (5 μm to 10 μm) in the hyperspectral images and it is based on the choice of the imaging sensor, and hence construct the images with very high spectral resolutions than the conventional multispectral images.

In general, hyperspectral images (HSI) are possessing high resolution and it is from decomposing the reflected sonar radiance into large number of bands with minor spectral resolutions, hence the spectra of the different land objects shows a nearly continuous shape (Liangpei and Du 2012). With hyperspectral images, classification of various land objects types inclusive of subclass types by mixing both the spectral and spatial information is possible. Currently this is the only technology having a such massive capacity and accurate classification and hence this technology is finding more and more users / researchers for different purposes (Landgrebe 2003; Liangpei and Du 2012; Tuia et al. 2015).

Latest trends and advances in hyperspectral remote sensing based forest tree classification have recently been summarized in Fassnacht et al. 2016. They reported that hyperspectral data tend to consider more species and result in higher accuracies. It has also been found that continuous spectral information contained in hyperspectral data seems even more suitable to differentiate tree species with similar spectral properties (Dalponte et al. 2012; Ghosh et al. 2014; Trier et al. 2018; Wietecha et al. 2019).

Hyperspectral sensors document the reflected electromagnetic energy from the surface of earth in the entire electromagnetic spectrum extending from the visible wavelength region through the near-infrared and mid-infrared region (0.3 μm to 2.5 μm) in tens to hundreds of narrow (in the order of 10 nm) contiguous bands. Such narrow bandwidths results in an almost continuous and comprehensive spectral response for each pixel giving precise and accurate information about its constituents and having an advantage over multispectral imaging.

Land cover, Land use maps produced from image classification are the most commonly used maps. These maps are mainly used for urban planning (Taubenböck et al. 2013; Jacobson et al. 2015), land development activities, agriculture surveys (Alcantara et al. 2012) or surveying of deforestation (Vaglio Laurin et al. 2014) etc. However, the quality of land cover maps is of prime importance and hence many researchers are working on image classification algorithms and their impact on the final maps, confirmed by ground reality (Plaza et al. 2009; Mountrakis et al. 2011; Camps-Valls et al. 2014; Linda and Strand 2014; Jacobson et al. 2015; Bradley et al. 2016). Improving the quality of maps derived from HSI is more important, as hyperspectral systems are often high dimensional (number of spectral bands acquired), spatially and spectrally correlated and affected by noise (Camps-Valls et al. 2014). The unique features that pose hyperspectral data challenges to image interpretation are mainly its higher dimensionality, the need for calibration and the redundancy in

the information. Generally land cover maps are smooth, in the sense that neighboring pixels tend to belong to the same type of land cover (Schindler 2012). But the spectral signatures of pixels of a same type of cover tend to become more and more uneven, especially with the increase of spatial resolution. Hence, hyperspectral imaging classification systems have the delicate task of describing a smooth land cover using spectral information with a high within-class variability.

However, the high spectral resolution of a hyperspectral sensor allows us to capture small deviations in the spectral response of the materials thus aiding in their identification. Several techniques viz., Artificial Neural network (ANN), SAM- Spectral Angle Mapper and SVM -Support Vector Machine; k-nearest neighbors (KNN), sparse representation and maximum likelihood etc. have been developed to analyze hyperspectral data (Hegde et al. 2014), which has advanced and well-organized classification algorithms. Besides different machine learning techniques are also available for classification. However in this study we have attempted SAM and SVM for landuse/landcover classification. By keeping all these information's, a study was initiated with the objective of analyzing how much efficiently a hyperspectral image can give information regarding the landuse/landcover within a specific area and comparing that with multispectral image.

Materials and methods

Study area and datasets

Kozhikode district lies between North latitudes 11° 08' and 11° 50' and East longitudes 75° 30' and 76° 8'. It is falling in parts of Survey of India Toposheets 58 A and 49 M. It is one of the coastal districts of Kerala. Kozhikode district is bounded on the north by Kannur district, on the east by Wayanad district, on the south by Malapuram district and on the west by Lakshadweep sea. The district can be divided into three geographical regions - highlands, midlands and low lands. Kozhikode has a humid tropical climate with a very hot season extending from March to May. The average annual rainfall for the district is 3438 mm. The maximum temperature in the month of May comes to 36 °C. Humidity is very high in the coastal region. Majority of the population of the district is dependent directly or indirectly on agriculture for their livelihood. The main crops grown in the district are **paddy**, **coconut**, **pepper**, **cashew**, **tapioca**, **arecanut** and plantation crops like **rubber**. Paddy occupies the largest area among annual crops, however a drastic reduction in paddy area occurred during the past decade. Being the first space borne hyperspectral instrument to acquire both visible near infrared and short wave infrared through two spectrometers and a single telescope, the data from EO-1 Hyperion had been used for this work. The high resolution hyperspectral image with a 30-m

resolution, is being provided by The Hyperion and it is having 220 spectral bands from 0.4 to 2.5 μm . The Hyperion provide detailed spectral mapping across all 220 channels with high radiometric accuracy and it can cover a land area of 7.5 km by 100 km per image.

In order to allow cross calibration, the last 20 bands of VNIR sensor are overlapping with the first 20 bands of SWIR sensor. For hyperspectral analysis, EO-1 Hyperion product: E01H1450522007049110PZ_1R from United States Geological Survey (USGS) contains data files either in Hierarchical Data Format (HDF) or Geographic Tagged Image-File Format (GeoTIFF) were used. Location map of the study area with the Hyperion image was provided in Fig. 1. Table 1 shows the details regarding the dataset attributes and data values.

Data processing methodology

The methodology included major steps as in Fig. 2. The objective of pre-processing is to make remotely sensed data amenable for efficient and reliable information extraction. As discussed in the introduction part, processing of hyper spectral image of high dimension is a difficult task and mainly the intricacy is a result of huge volume of data in abundant spectral bands. Besides, sensor and atmospheric noise needs

Table 1 Hyperion data set attributes and attribute values

Data Set Attribute	Attribute Value
Entity ID	EO1H1450522007049110PZ_SGS_01
Acquisition Date	2007/02/18
Cloud Cover	10% to 19% Cloud Cover
Orbit Path	145
Orbit Row	52

to be reduced / minimized to arrive at a useful data and information, since Hyperion operates from a space platform with modest surface signal levels and a full column of atmosphere attenuating the signals. Specifically, the Hyperion dataset had to be pre processed for abnormal pixels, striping and smiling prior to the atmospheric correction. Mainly pre-processing of these images is done to remove errors occurred during acquisition by the sensor and selection of bands to reduce the data dimensionality and to minimize the complexity in the computation. Once the preprocessing stage is over, the Hyperion image is classified using Spectral Angle Mapper and Support Vector Machine techniques as in Fig. 2. For this work, the Hyperion data analysis and classification had done through image processing software ENVI 5.0.

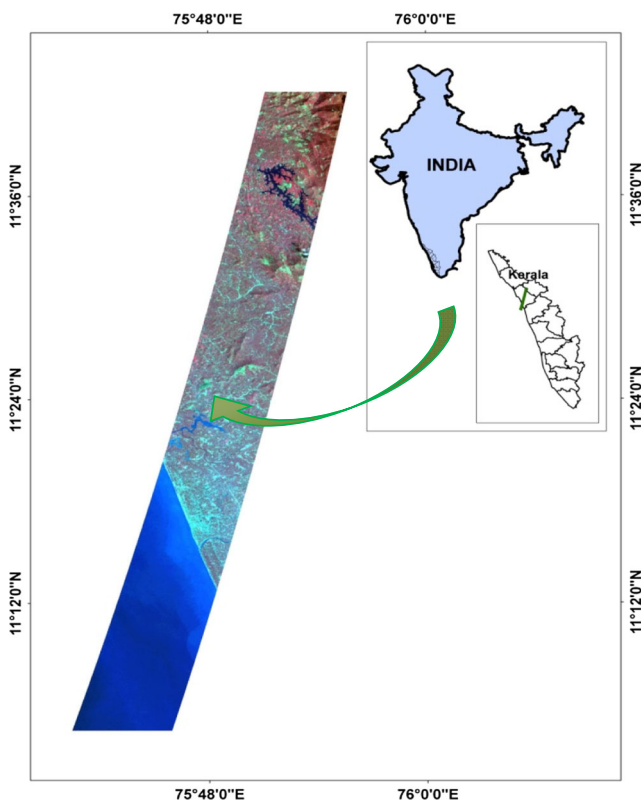


Fig. 1 Location Map of the study area with the Hyperion Image

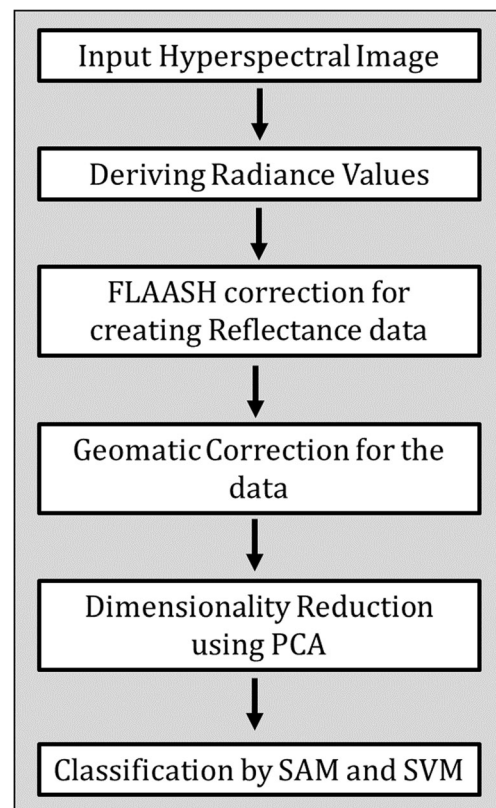


Fig. 2 Work flow in Step 1

The Hyperion EO-1 L1R (L1R-Level 1 Radiometric) product from the United States Geological Survey (USGS) website, for the study region had been acquired and it contain altogether 220 bands, however, calibration was done for only 196 bands. This is because merely 196 unique channels could be found since there is an overlap between the VNIR and SWIR focal planes (Beck 2003). The specific bands are 8–57 for the VNIR and 79–224 for the SWIR, which have been selected manually and used for calibration. The reason for not calibrating all 220 channels is mainly due to the detectors' low responsivity. For retrieving reflectance values, atmospheric correction was applied to the resized data using Fast Line-of-sight Atmosphere Analysis of Spectral Hypercube (FLAASH) as adopted in the ENVI package. After FLAASH, bands having low reflectance values were removed manually, which made the number of bands to 145.

Geometric correction of the data

For the accurate classification, the data should be geometrically corrected. Nowadays, the data from many sensors are captured with comprehensive information such as details of acquisition, platform geometry etc., it will help in geometric rectification using models and for the registration of maps. In order to rectify the Hyperion image, a geo-referenced IRS-P6 LISS III image of the study area has been used as the reference image. The projection for the study area is UTM at Zone 43(North) and Datum: WGS84.

Dimensionality reduction

For the application of land-use or land-cover mapping the objective may be to use supervised or unsupervised classification of the hyperspectral image, which, implies that it is not essential that the categorization is implemented in the spectral space. However, since there is a difficulty in verification of entire ground truth, low-dimensional feature space image classification may be preferred. There are several statistical techniques viz., principal component analysis (PCA), minimum noise fraction transformation or independent components rotation, which will aid in classification. For this work, band reduction was achieved with Principal Component Analysis. PCA is a statistical technique, which is used to highlight the variations in the datasets and bring out well-built patterns in a dataset. Mainly this will help to explore the data in different forms and also to visualize the same.

In short, PCA smooth the progress of the simplification of large data sets. The data will be transformed orthogonally to change a set of observations of possibly correlated variables into a set of uncorrelated variables (linearly values) called principal components (Vidhya et al. 2014). This is done by identifying a new position of orthogonal axes that have their source at the data mean and are changed to a new coordinate

system so that the spectral variability is maximized. This will result in PC bands of linear combinations of the unique original spectral bands and are uncorrelated. In this technique, It is feasible to calculate the same number of output PC bands as input spectral bands. The output will have the largest percent of data variance for the first PC band and the second PC band contains the second largest data variance, and likely to continue in such a way. The last and few final PC bands will be noisy since they contain very small variance, much of which is due to noise in the original unique spectral data. The resultant PCA bands will have more colorful color composite images than spectral color composite images since the data is uncorrelated. The software ENVI can be used to complete forward and inverse PC rotations.

Classification by SAM and SVM

ENVI software was used for the classification of the Hyperion data. Area of interests of each specific class was given using the ROI tool. Barren land, Reserved forests, Settlement, Rock exposure, Coconut, Rubber plantation, Crop land, Water body and Coconut dominant mixed crop are the classes considered in the study region. The classification algorithms used are SAM and SVM. Spectral Angle Mapper (SAM) uses an n-D angle to match pixels to reference spectra and it is based on a physical spectral classification (Kruse et al. 1993). This technique matches up to the angle between the endmember spectrum vector and each pixel vector in n-D space. Smaller angles represent closer matches to the reference spectrum. Pixels which are away than the particular maximum angle threshold in radians are usually not classified. This technique is comparatively insensitive to albedo effects and light (illumination) when used on final calibrated reflectance data. Endmember spectra used by SAM will be derived from spectral libraries or ASCII files, or can be extracted directly from an image (as ROI average spectra). The spectral angle is calculated using the following equation,

$$\theta = \cos^{-1} \left(\frac{\sum_{i=1}^n t_i r_i}{\sqrt{\sum_{i=1}^n t_i^2 \sum_{i=1}^n r_i^2}} \right) \quad (1)$$

Where,

- n is the number of spectral bands,
- r as the reflectance of the reference spectrum and
- t is the reflectance of the actual spectrum

Another method used in the study is, the Support Vector Machine (SVM), which is also a classification method of remote sensing images based on the statistical

information (Corinna and Vladimir 1995). This is a supervised classification method results in good classification results from complex and noisy data by using statistical learning theory. This method distinguishes the classes with a decision surface that take full advantage of the margin between the classes. The surface is termed as optimal hyperplane, and the points of data closest to the hyperplane are named as support vectors. These support vectors are the vital elements of the training set. SVM comprises a penalty parameter that permits a certain degree of misclassification, which is predominantly important for non-separable training sets. This penalty parameter controls the trade-off between training errors allowed and forced rigid margins. It creates a soft margin that allows some misclassifications, such as some training points on the wrong side of the hyper plane. If the value of the penalty parameter is increased means then that will escalate the errors in misclassifying points and forces the creation of a more accurate model that may not generalize well. As same as in SAM, using ROI Tool in ENVI Classic, training regions was defined for each class.

Results and discussions

Selecting informative bands

The Hyperion data contain 220 bands at the initial stage. It is through several processing steps, the bands having more information are selected. Figure 3 shows separate spectral profiles for the nine different classes selected for the current study. Atmospheric correction method, FLAASH were used to achieve the reflectance values from the same, wherever the downloaded data have radiance values. The following Fig. 4 shows the output after each pre-processing stages of the Hyperion image i.e. from the downloaded data to the stage of dimensionality reduction by PCA.

Geometric correction of image

In order to rectify the Hyperion image, a georeferenced IRS-P6: LISS III image of the study area acquired by USGS has been used as the reference image. The projection for the study area is UTM at Zone 43(North) and Datum: WGS84.

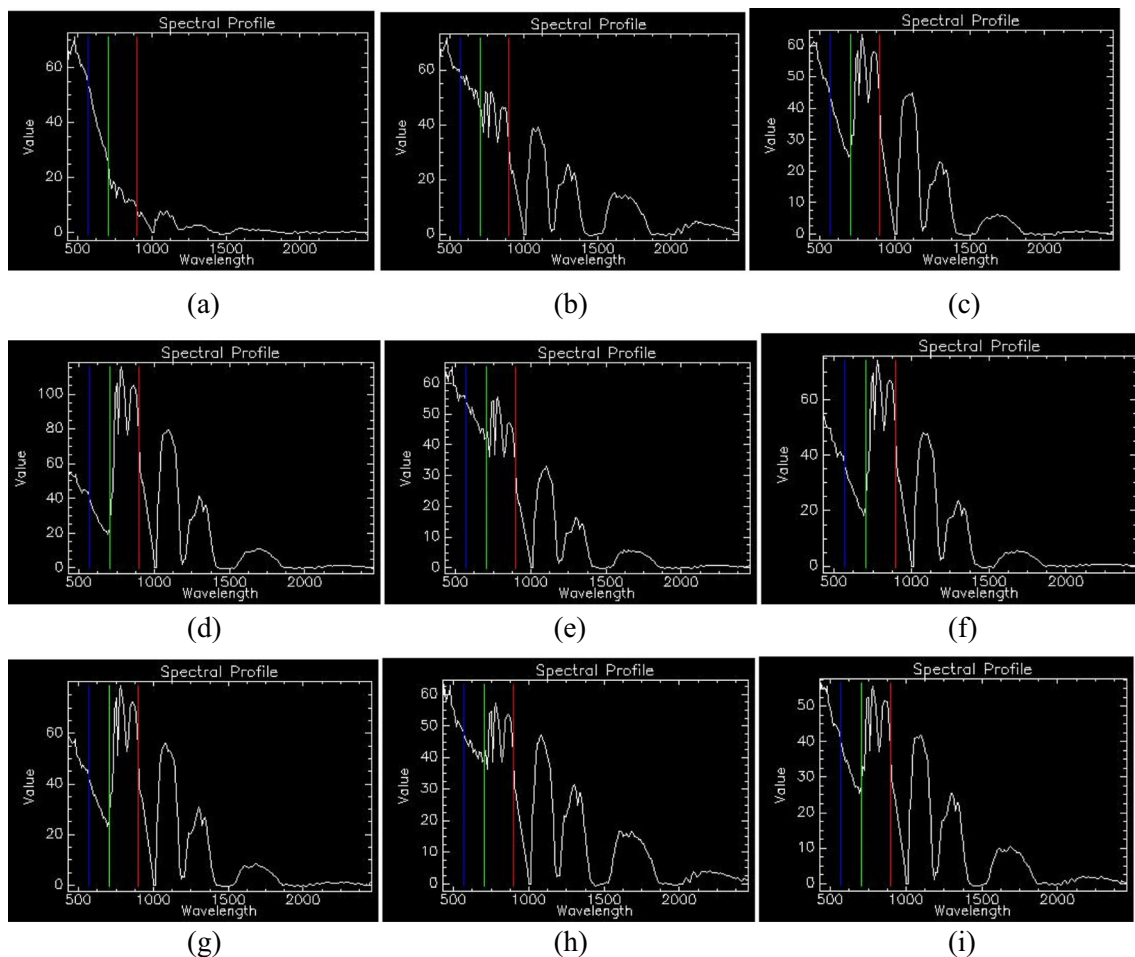
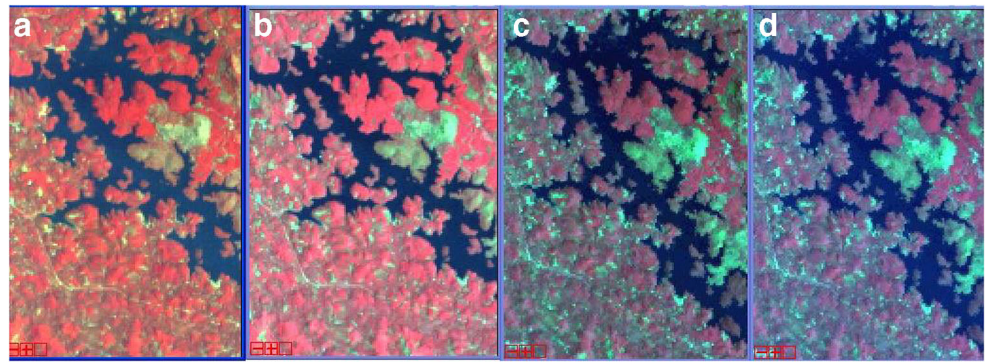


Fig. 3 Spectral profiles for the nine different classes (a) Water body (b) Settlement (c) Coconut (d) Rubber plantation (e) Crop land (f) Reserved Forests (g) Coconut dominant mixed crop (h) Barren land (i) Rock exposure

Fig. 4 **a** Hyperion FCC **b** Hyperion after FLAASH **c** Hyperion after Geometric Correction **d** Hyperion after PCA



Undergoing SAM and SVM classification

An effort was made to classify dimensionality reduced hyperion image using SAM and SVM. SAM and SVM algorithm were used for classification initially with the training samples directly selected from the image. Some sample sites which are representative were recognized covering nine major land cover classes existing in the study area. The land cover classes included Barren land, Reserved forests, Settlement, Rock

exposure, Coconut, Rubber plantation, Crop land, Water body and Coconut dominant mixed crop.

The Fig. 5 shows the classified output image for both SAM and SVM. SVM classifier performed much better than SAM classifier. When compared, different land use classes of the study area derived using SAM was unsuccessful in spatially depicting the specific land use. Even if there are nine classes distinguished at the output stage, percent of each classified class is different in both. Table 2 shows the percentage of

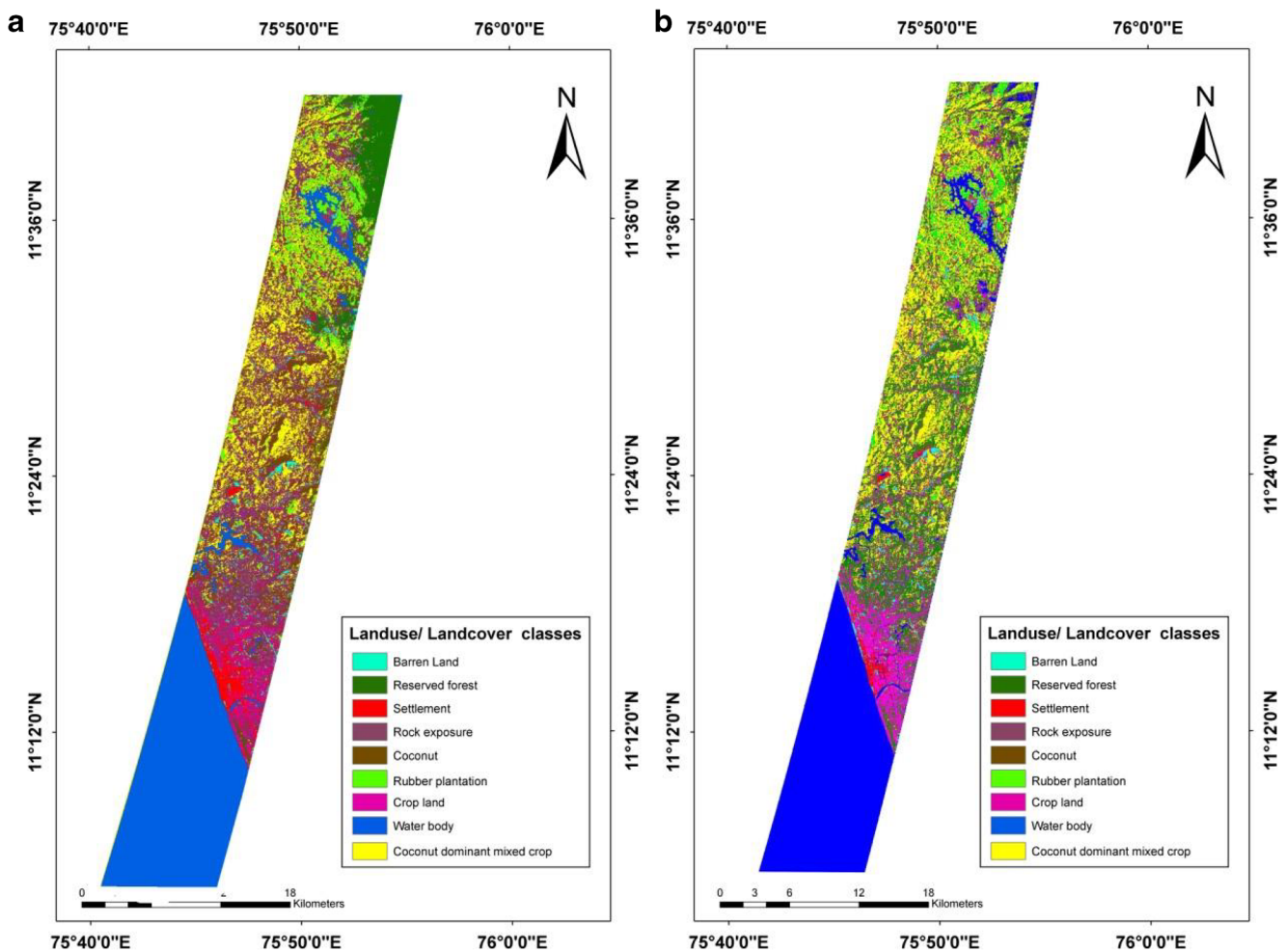


Fig. 5 **a** SVM classified Hyperion **b** SAM classified Hyperion

Table 2 Percent of SVM and SAM classification for hyperion data

Land use Classes	Percent of classification in SVM (%)	Area covered in hectares	Percent of classification in SAM (%)	Area covered in hectares
Unclassified	0	0	68.63	96629.41
Barren land	0.56	798.3472	0.63	898.9344
Reserved forest	1.97	2786.022	5.89	8297.778
Settlement	0.82	1227.509	0.47	662.7152
Rock exposure	7.16	10089.84	3.55	5001.136
Coconut	3.70	5217.990	0.82	1158.517
Rubber plantation	1.74	2455.880	1.25	1770.586
Cropland	1.43	2016.997	1.99	2807.739
Water body (in land +sea)	9.50	13457.83	9.82	13843.40
Coconut dominant mixed crop	72.97	102740.1	6.90	9720.267

classification performance for the Hyperion data. The main limitation of SAM method of classification is the unclassified pixels within the spectral angle threshold of 0.12 rad. The SVM classifier was able to classify major land use classes including Coconut, Crop land, Rock exposure and Reserved forests more specifically and accurately whereas the SAM classification showed it poor.

Similarly, the landuse/landcover classes like Settlement and Barren land could be uniquely delineated in SVM. The classification result was verified with the data collected from ground truth. Table 3 shows the overall accuracy and the kappa coefficient calculated for the SVM and SAM classifiers. Table 3 describes the superiority of SVM over SAM. The overall accuracy measured are 85.6% and 64.7% for SVM and SAM, and the kappa coefficient calculated is as 0.89 for SVM and 0.60 for SAM, respectively. In SAM, the spectral confusion in pixels while choosing the end members from the image led to underestimation and overestimation errors.

Apart from this, the main advantage of SVM over SAM is its ability to work with smaller training samples. The major reason which may be attributed for this precise classification accuracy of landuse/landcover classes by SVM is the fact that this classifier has been designed in such a way to identify an

Table 3 Classification performance of SVM and SAM

	Overall Accuracy (%)	
	SVM	SAM
Overall	85.6	64.7
Kappa	0.89	0.60

optimal hyper plane for class separation (George et al. 2012). The SVM algorithm is sensitive to the size of training set and dimensionality of the data set. The SVM is a supervised non-parametric classification algorithm based on statistical learning theory. It provides some system-inherent advantages in comparison to other classification algorithms. Possibly the aforementioned points yields good classification results from complex and noisy data by SVM method. However, the reason for the poor output of SAM may be due to higher variation in reflectance values of classes.

Conclusion

The present study was to explore how efficiently a hyperspectral data like Hyperion can be more informative for landuse/landcover classification. The pre-processing steps for Hyperion data included atmospheric correction using MODTRAN based FLAASH module and Principal Component Analysis (PCA) for data dimensionality reduction. Using the training samples from the image itself, advanced classifiers like Support Vector Machine (SVM) and Spectral Angle Mapper (SAM) made the classification of landuse/landcover classes for the Hyperion. The landuse/landcover classes included Barren land, Reserved Forests, Settlement, Rock exposure, Coconut, Rubber plantation, Crop land, Water body and Coconut dominant mixed crop. SVM classifier showed more specific and consistent result with higher precision classification and more accuracy indicating its superior performance in classification of landuse/landcover. SAM resulted in more unclassified pixels and poor classification accuracy. The present study indicated the potential of hyperspectral data in providing more spectral information by classifying a specific area with nine landuse/landcover classes.

Acknowledgements The authors are thankful to Executive Director, CWRDM for her constant encouragement and the necessary support during the entire study period. Financial support from CWRDM plan fund as Research funding is gratefully acknowledged.

References

Alcantara C, Kuemmerle T, Prishchepov AV, Radeloff VC (2012) Mapping abandoned agriculture with multi-temporal MODIS satellite data. *Remote Sensing Environment*. 124:334–347

Beck R (2003). EO-1 user guide, version 2.3, University of Cincinnati, satellite systems branch, USGS earth resources observation systems data Centre (EDC)

Bradley AV, Isabel MDR, Pontius Jr. RG, Ahmed ES, Araújo MB, Brown D, Brandão Jr. A, Câmara G, Tiago GSC, Hartley AJ, Smith MJ and Ewers R (2016) SimiVal, a multi-criteria map comparison tool for land use change model projections. *Environmental Modelling and Softwares*. 82, 229–240

- Camps-Valls G, Tuia D, Bruzzone L, Benediktsson JA (2014) Advances in hyperspectral image classification. *IEEE Signal Process Mag* 31: 45–54
- Corinna C, Vladimir V (1995) Support-vector networks. *Mach Learn* 20: 273–297
- Dalponte M, Bruzzone L, Gianelle D (2012) Tree species classification in the southern Alps based on the fusion of very high geometrical resolution multispectral/hyperspectral images and LiDAR data. *Remote Sens Environ* 123:258–270. <https://doi.org/10.1016/j.rse.2012.03.013>
- Fassnacht FE, Latifi H, Stereńczak K, Modzelewska A, Lefsky M, Waser LT, Straub C, Ghosh A (2016) Review of studies on tree species classification from remotely sensed data. *Remote Sens Environ.* <https://doi.org/10.1016/j.rse.2016.08.013>
- George PP, Arvanitis K and Sigrimi N (2012). Hyperion hyper spectral imagery analysis combined with machine learning classifiers for land use/cover mapping. *Expert System with Applications* 39, 3800–3809
- Ghosh A, Fassnacht FE, Joshi PK, Koch B (2014) A framework for mapping tree species combining hyperspectral and LiDAR data: role of selected classifiers and sensor across three spatial scales. *Int J Appl Earth Obs Geoinform* 26:49–63. <https://doi.org/10.1016/j.jag.2013.05.017>
- Hegde G, Ahamed JM, Hebbar R and Raj U (2014). Urban land cover classification using hyper spectral data, ISPRS technical commission VIII symposium, *The International archives of the Photogrammetry, Remote Sensing and Spatial Information Sciences*. Vol. XL-8, 751–754
- Jacobson A, Jasjeet D, Jessie G, Hannah J, Zoe R, Stanish AH (2015) A novel approach to mapping land conversion using Google earth with an application to East Africa. *Environ Modell Softw* 72:1–9
- Kruse F A, Lefkoff A B, Boardman JW (1993) The Spectral Image Processing System (SIPS) – Interactive Visualization and Analysis of Imaging Spectrometer Data, *Remote Sen Environ* 44:145–163
- Landgrebe DA (2003) *Signal theory methods in multispectral remote sensing*. Wiley-Interscience, New York
- Liangpei Z, Du B (2012) Recent advances in hyper spectral image processing. *Geo-spatial Inform Sci* 15(3):143–156
- Lillesand TM, Kiefer RW, Jonathan CW (2009) *Remote sensing and image interpretation*, fourth edn. Wiley, New York
- Linda AL, Strand GH (2014) Comparison of variance estimation methods for use with twodimensional systematic sampling of land use/land cover data. *Environ Modell Softw* 61:87–97
- Liu B, Zhang L, Zhang X, Zhang B, Tong Q (2009) Simulation of EO-1 Hyperion Data Based on the Spectral Reconstruction Approach. *Sensors*:1424–8220
- Mountrakis G, Ima J, Ogole C (2011) Support vector machines in remote sensing: a review. *ISPRS J Photogramm Rem Sens* 66(3):247–259
- Ndehedehe CE, James EE (2013) Assessment of spectral angle mapper and binary encoding in the quantification of the built environment from multi-spectral Landsat imagery. *New York Sci J* 6(9):107–111
- Plaza A, Benediktsson JA, Boardman J, Brazile J, Bruzzone L, Camps-Valls G, Chanussot J, Fauvel M, Gamba P, Gualtieri A, Marconcini M, Tilton JC, Trianni G (2009) Recent advances in techniques for hyperspectral image processing. *Remote Sens Environ* 113(Supplement 1):S110–S122
- Schindler K (2012) An overview and comparison of smooth labeling methods for land-cover classification. *IEEE Trans Geosci Remote Sens* 50(11):4534–4545
- Taubenböck H, Klotz M, Wurm M, Schmeider J, Wagner B, Wooster M, Esch T, Dech S (2013) Delineation of central business districts in mega city regions using remotely sensed data. *Remote Sens Environ* 136:386–401
- Trier ØD, Salberg AB, Kermit M, Rudjord Ø, Gobakken T, Næsset E, Aarsten D (2018) Tree species classification in Norway from airborne hyperspectral and airborne laser scanning data. *Eur J Remote Sens* 51:336–351. <https://doi.org/10.1080/22797254.2018.1434424>
- Tuia D, Flamari R, Nicolas C (2015) Multiclass feature learning for hyperspectral image classification: Sparse and hierarchical solutions. *ISPRS J Photogramm Remote Sens* 105:272–285
- Vaglio Laurin G, Chen Q, Lindsell JA, Coomes DA, Del Frate F, Guerriero L, Pirotti F, Valentini R (2014) Above ground biomass estimation in an African tropical forest with lidar and hyperspectral data. *ISPRS J Photogramm Remote Sens* 89:49–58
- Vidhya R, Vijayasekaran D, Farook MA, Jai S, Rohini M, Sinduja A (2014) Improved classification of mangroves health status using hyper spectral remote sensing data. *International Archives of the Photogrammetry, Remote Sensing and Spatial Information Sciences* XL-8:667–670
- Wietecha M, Jełowicki Ł, Mitelsztedt K, Stereńczak K, Miścicki S (2019) The capability of species-related forest stand characteristics determination with the use of hyperspectral data. *Remote Sens Environ*:231. <https://doi.org/10.1016/j.rse.2019.111232>

Publisher's note Springer Nature remains neutral with regard to jurisdictional claims in published maps and institutional affiliations.